Supplementary information

Prp2-mediated protein rearrangements at the catalytic core of the spliceosome as revealed by dcFCCS

Thomas Ohrt [1,3], Mira Prior [2,3], Julia Dannenberg[1], Peter Odenwälder[1], Olexandr Dybkov[1], Nicolas Rasche[1], Jana Schmitzová[1], Ingo Gregor[2], Patrizia Fabrizio[1], Jörg Enderlein[2,4] and Reinhard Lührmann[1,4]

1) Max Plank Institute for Biophysical Chemistry. Göttingen, Germany
2) III. Physikalisches Institut (Biophysik). University of Göttingen, Germany

[3] These authors contributed equally to this work.
[4] Corresponding authors

Inventory of Supplementary information

Supplementary information

Supplementary Fig. 1

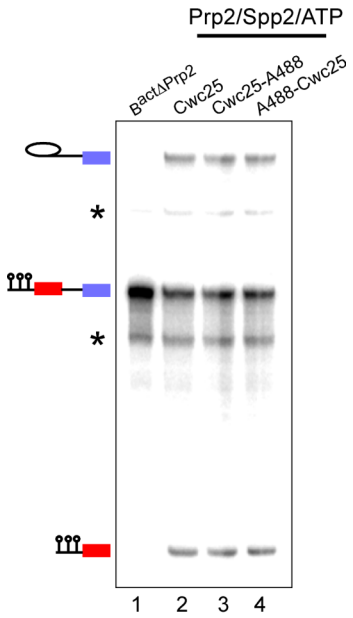

Fig. S1. Complexes assembled on Atto647N-M3Act undergo the first step of splicing when complemented with Prp2, Spp2, ATP and Cwc25 labelled with the fluorescent dye Alexa488. $B^{actΔPrp2}$ complexes assembled on Atto647N-M3Act (lane 1) were purified, eluted from the amylose matrix and complemented with Prp2, Spp2, ATP and Cwc25 (lane 2), or fluorescently labelled Cwc25 (lanes 3 and 4). Two preparations of Cwc25, C-terminally (lane 3) and N-terminally labelled (lane 4) were used. RNA was analysed on an 8% polyacrylamide–urea gel and visualised by autoradiography. The positions of the pre-mRNAs and the splicing intermediates are indicated on the left. Asterisks: uncharacterised pre-mRNA bands.

Supplementary Fig. 2

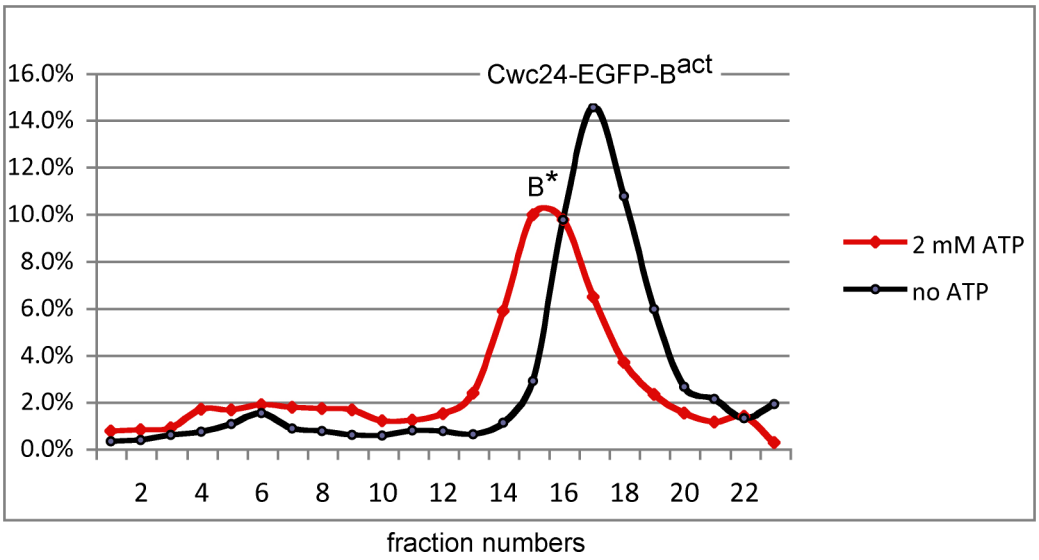

Fig. S2. Catalytic activation of the Cwc24-EGFP–B^{actΔPrp2} complex by Prp2. Profile of affinity-purified Cwc24-EGFP–B^{actΔPrp2} spliceosomes separated on a glycerol gradient containing 75 mM KCl after incubation with Prp2/Spp2 without the addition of ATP (45S; black line) or with the addition of 2 mM ATP (40S, B* complex; red line). The radioactivity contained in each gradient fraction was measured by Cerenkov counting. Sedimentation coefficients were determined by analysing the UV absorbance of fractions of a reference gradient containing prokaryotic ribosomal subunits. The y axis shows the percentage of radioactively labelled RNA found in each fraction relative to the amount found in all fractions.

Supplementary Fig. 3

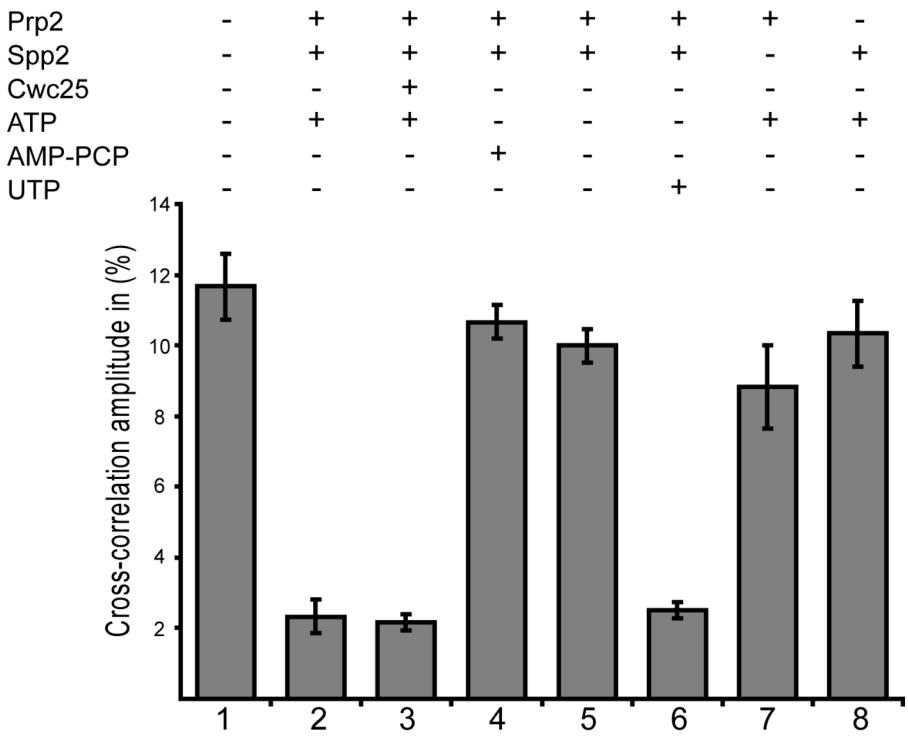

Fig. S3. Binding of Cwc27-EGFP fusion protein to the spliceosome analysed by dcFCCS. Affinity-purified $B^{act\Delta Prp2}$ complexes assembled on Atto647N-M3-act wt, carrying Cwc27-EGFP (column 1), were complemented as indicated above each bar. dcFCCS measurements were then performed at complex concentrations of 1.0 nM and the observed cross-correlation amplitudes were corrected for background. Cross-correlation amplitudes derived from two independent measurements are plotted against the respective complex. Error bars indicate the standard deviation of two independent measurements.

Supplementary Fig. 4

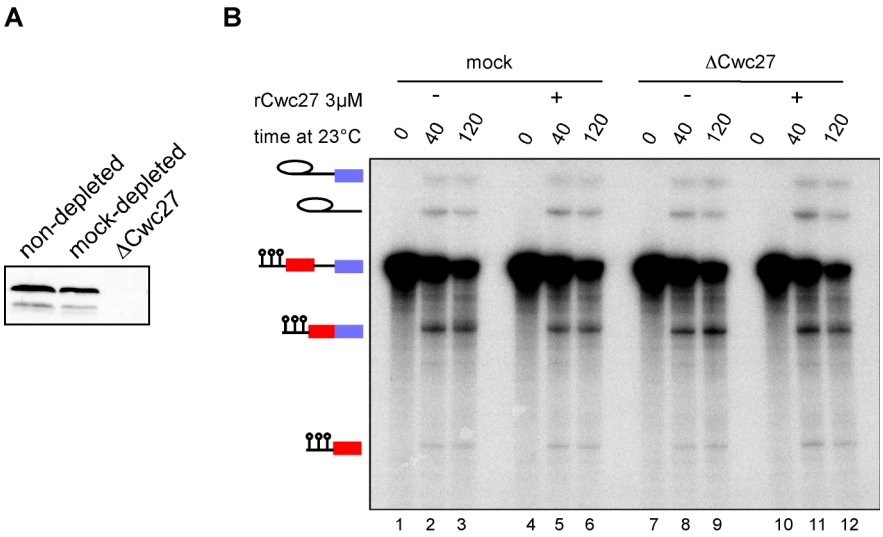

Fig. S4. Cwc27 is dispensable for step 1 of splicing *in vitro*. (A) Western blot analysis of yeast splicing extracts carrying Cwc27 tagged with the TAP tag before and after depletion of Cwc27 (ΔCwc27) (B) M3Act pre-mRNA was incubated in yeast whole-cell extract, which was either mock- (lanes 1–6) or Cwc27-depleted (lanes 7–12). Recombinant Cwc27 was then added to a final concentration of 3 μM. The splicing mixtures were incubated at 23 °C and stopped at the time indicated. RNA was analysed on an 8% urea–polyacrylamide gel and visualised by autoradiography. The positions of the pre-mRNAs, the splicing intermediates and products are indicated on the left.

Supplementary Materials and Methods

Strains and plasmids

To construct yeast strains with the yEGFP tag at the C terminus of selected proteins, the yEGFP cassette was amplified by PCR from the plasmid pKT209 (purchased from Euroscarf, Frankfurt am Main). We used this PCR product to transform haploid yeast cells from strain 3.2.AID/CRL2101 (Yean and Lin, 1991), and transformants were selected on synthetic dextrose dropout medium lacking uracil. The correct integration of the tag in the genome was confirmed by PCR, and on the protein level by western blotting. The resulting strains carry a single chromosomal copy of the gene of interest, containing the yEGFP tag, the Candida albicans URA3 marker at their C terminus and in addition a temperature-sensitive Prp2 ATPase (*prp2-1*). The construction of the yeast strain expressing TAP-tagged Cwc24 was performed as described for yEGFP-tagging using the plasmid pBS1539 (Puig et al., 2001). Primer sequences for yEGFP and TAP tagging are available upon request. Strains containing the yEGFP and the TAP tag used in this work are summarised below.

In vitro splicing and purification of $B^{act\,\Delta prp2}$ spliceosomes

Extracts were prepared from the yeast strains listed below. Yeast cultures were grown at 25°C to OD_{600} 3–5 and the extract were heat-inactivated for 30 min at 35°C prior to *in vitro* splicing reactions. Splicing reactions (6 to 36 ml) were incubated for 30–40 min at 23°C with 1.8 nM Atto647N-M3Act wild-type pre-mRNA. To facilitate tracking during spliceosome purification, a fraction of the M3Act pre-mRNA was co-transcriptionally ^{32}P-labelled (specific activity: 7.000–10.000 cpm/fmole) and mixed with unlabelled Atto647N-M3Act pre-mRNA to give a specific activity of 50–60 cpm/fmole for dcFCCS experiments and 800 cpm/fmole for splicing experiments, respectively. The complexes were purified using the procedure described previously (Fabrizio et al., 2009; Warkocki et al., 2009).

Gel analysis

After the splicing reaction, samples were treated with proteinase K, extracted with phenol-chloroform and precipitated with 3 volumes of ethanol. RNAs were separated by electrophoresis on 8% polyacrylamide gels (29:1, polyacrylamide:bisacrylamide)

containing 8M urea (UREA-PAGE) and exposed to a Phosphorimager screen (Amersham) or autoradiography.

Dual-colour fluorescence cross correlation spectroscopy (dcFCCS)

dcFCCS allows for the analysis of molecular interactions such as binding or release of proteins in a complex system (Kettling et al., 1998; Földes-Papp and Rigler, 2001; Ohrt et al., 2011). dcFCCS requires particles labelled with two spectrally separated colours (e.g. green and red). The fluorescence of the labelled molecules is spectrally separated and detected in two channels. The signals are analysed by computing the auto-correlation of each channel and their cross-correlation. If molecules bearing different labels are not part of the same complex, then they will diffuse independently through the confocal volume. In that case, there will be no cross-correlation between both signals. However, if the molecules are part of the same complex, they will form doubly labelled entities. Co-diffusion of the two labels will generate correlated signals in both detection channels and therefore a cross-correlation. The amplitude of the cross-correlation is proportional to the number of doubly labelled molecules and can therefore be used to monitor binding and release reactions (Ricka and Binkert, 1989; Schwille et al., 1997; Földes-Papp, 2005; Mütze et al., 2011).

Set-up

The dual-colour-FCCS setup (MicroTime 200, PicoQuant GmbH, Berlin, Germany) is based on an inverse epi-fluorescence microscope (IX-71, Olympus Europa, Hamburg, Germany). The system is equipped with two identical pulsed 470 nm diode lasers (LDH-P-C-470 B, PicoQuant GmbH, Berlin, Germany) and two identical pulsed 635 nm diode lasers (LDH-P-635, PicoQuant GmbH, Berlin, Germany) with linear polarisation and a pulse duration of 50 ps (FWHM). The lasers are pulsed alternately with an overall repetition rate of 40 MHz (PIE mode) corresponding to a delay between pulses of 25 ns (PDL 828 “Sepia II”, PicoQuant GmbH, Berlin, Germany). The light of each of the two pairs of identical wavelength but crossed polarisation lasers is combined by two polarising beam splitters (Ealing Catalogue, St. Asaph, UK) into single beams. These beams are combined by a dichroic mirror (490 dcxr, Chroma Technology, Rockingham, VT, USA) resulting in a single beam containing both wavelengths. The beam is coupled into a polarisation-preserving single-mode fibre. At the fibre output, the light is collimated and reflected towards the

objective by a dichroic mirror (FITC/TRITC, Chroma Technology, Rockingham, VT, USA). The light is focused by the microscope's objective (UPLSAPO 60x W, 1.2 N.A., Olympus Europa, Hamburg, Germany). Fluorescence is collected by the same objective (epi-fluorescence mode), passed through the dichroic mirror, and focused by a tube lens through a single circular aperture (diameter 150 μm). After the pinhole, the light is re-collimated, split by a polarising beam splitter cube (Ealing Catalogue, St. Asaph, UK) and two dichroic mirrors (640 dcxr, Chroma Technology, Rockingham, VT, USA), and focused onto two single photon avalanche diodes for the red (two SPCM-AQR-13, Perkin Elmer, Wellesley, MA, USA), and two for the green emission (PDM 50-C, Micro Photon Devices, Milan, Italy), respectively. This kind of excitation/emission scheme yields maximum information on fluorescence anisotropy and spectrum, although we sebsequently use only the spectral information. Emission bandpass filters HC692/40 and HC520/35 (Semrock, USA), positioned directly in front of each detector, are used for blocking scattered light. A time-correlated single-photon counting electronics (HydraHarp 400, PicoQuant GmbH, Berlin, Germany) independently records the detected photons of all detectors with an absolute temporal resolution of 4 ps on a common time frame.

Computation and evaluation of the correlation data

All correlation curves are calculated by a dedicated software algorithm (Wahl et al., 2003). In a first step, one calculates the following: the autocorrelation functions (ACFs) of the focal volumes excited by the first green laser (GG_1), the second green laser (GG_2), the first red laser (RR_1), and the second red laser (RR_2). Furthermore, one needs the corresponding cross correlation functions between both green (GG_X) and both red (RR_X) focal volumes. In the same way, one computes the correlation functions for photon pairs of which the first photon was excited by the first green laser and the second was excited by the first red laser (GR_1), and accordingly GR_2, RG_1, RG_2, GR_X, and RG_X. Since the laser settings and buffer conditions are always constant during one set of experiments, a blank measurement is done using just the buffer as sample. The computation of the correlation data in absolute units of cps² allows to compensate for the buffer background by simple subtraction of the corresponding blank curves. In this way, one can reduce the number of data for the subsequent data evaluation by setting $G_n = GG_n - GG_n^0$, $R_n = RR_n - RR_n^0$, and $M_n = (GR_n - GR_n^0 + RG_n - RG_n^0) / 2$ (where n can take the values {1, 2, and X} and

the index 0 denotes the corresponding data of the blank sample). These three sets of data are each fitted independently by a global fit using a standard model based on a appropriate approximation of the molecule detection function (Dertinger et al., 2007). Most generally, one finds three types of molecules in solution: A fraction (*g*) that carries only the green label, a second fraction that carries only the red label (*r*), and a fraction of complexes that carry both labels (*m*). From the fits of the correlation curves one obtains the diffusion constant of the molecules, the amplitude a_n^c of the diffusion term, and the uncorrelated intensity contribution b_n^c for each curve. Here *n* stands for the focal volume {1, 2, or X} and *c* for the observed colour {G, R, M}. FCS theory predicts that the relative amplitude $\gamma_n = b_n^G / a_n^G$ is equal to the number of molecules within the focal volume carrying a green label

$$\gamma_n = \frac{b_n^G}{a_n^G} = N_n^g + N_n^m$$

where N_n^g and N_n^m are the average number of green and mixed-coloured molecule in the *n*th detection volume, respectively. Similar relations hold for the red and mixed colours:

$$\rho_n = \frac{b_n^R}{a_n^R} = N_n^r + N_n^m$$

$$\mu_n = \frac{a_n^M}{b_n^M} = \frac{N_n^m}{\left(N_n^g + N_n^m\right)\left(N_n^r + N_n^m\right)}$$

Typically, the focal volumes for the different colours do not have the same size. Therefore, one cannot directly solve these equations for the different numbers of molecules. Instead, one needs to calibrate the focal volumes. For that purpose, a dilute sample of doubly labelled dsDNA (25-25 bases, FCCS Standard Probe, IBA GmbH, Göttingen, Germany) is measured as reference. Since this sample shows perfect co-diffusion for all colours, one knows *a priori* that $\tilde{N}_n^g = \tilde{N}_n^r = 0$ (all symbols with ~ denotes the reference sample). In case of identical volumes, one would expect to find $\tilde{\gamma}_n = \tilde{\rho}_n = 1/\tilde{\mu}_n$. For the actual, non-identical volumes, one introduces the calibration factors $c_n^g = 1/\tilde{\gamma}_n\tilde{\mu}_n$ and $c_n^r = 1/\tilde{\rho}_n\tilde{\mu}_n$. For the overlap between the red and the green excitation/detection volume, the average number of molecules is then given by the simple relations $N_n^g = c_n^g\gamma_n - N_n^m$, $N_n^r = c_n^r\rho_n - N_n^m$, and $N_n^m = \mu_n c_n^g\gamma_n c_n^r\rho_n$.

Hill fitting

Data points were fitted using the Hill equation

$$y = \frac{x^n}{K_d^n + x^n} + C$$

where y is the cross-correlation amplitude, x the complex concentration, n the Hill coefficient, K_d the binding constant and C a constant taking into account some offset in the cross-correlation amplitude. For the fitting, we set n equal to one, assuming a non-cooperative one-to-one binding behaviour. The mean K_d and its error were estimated by a bootstrapping method taking into account the standard deviation of each data point (Boos, 2003).

Expression and purification of Prp2, Spp2, Cwc24, Cwc25 and Cwc27

Recombinant Prp2, Spp2, Cwc24, Cwc25 and Cwc27 were expressed in *E. coli* and purified essentially as described previously (Warkocki et al., 2009).

Labelling of Cwc25

Cwc25 does not contain any cysteine in its amino acid sequence. For fluorescent labelling we added MGAC to the N- and/or a single cysteine at the C-terminus. The DNA sequence of either construct was confirmed by sequence analysis. The cysteine mutants, Cwc25-N, Cwc25-C and Cwc25-N/C, were labelled with the fluorescent reagent Atto488-maleimide (Atto-Tec). The labelling was performed in 100 mM $NaPO_4$-buffer (pH 7.2) which contained 10 μM reducing agent tris(2-carboxyethyl)phosphine (TCEP) (Sigma). The reaction mixture contained 20 *n*M protein and 2mM Atto488-maleimide, which was added in DMF. The reaction was allowed to proceed at 20°C for 2h. The reaction was stopped by adding GSH. Excess of the reagents was removed by gel filtration on a PD10 gel filtration column equilibrated with GK75. The degree of labelling was calculated according to the manufacturer protocol (Jena Bioscience) and yielded 73% of labelled Cwc25 at the C-terminus and 51% at the N-terminus and 57% of Cwc25-N/C.

List of yeast strains

3.2.AID *MATalpha*; *prp2-1; ade2; his3; lys2-801; ura3,* (carrying a G360D substitution in the helicase domain of Prp2)(Yean and Lin, 1991)

YTO13 Snu114-yEGFP
MATalpha, *prp2-1, ade2, his3, lys2-801, ura3*; *SNU114*::yEGFP-Ca*URA3* C-terminus

YTO15 Cus1-yEGFP
MATalpha, *prp2-1, ade2, his3, lys2-801, ura3*; *CUS1*::yEGFP-Ca*URA3* C-terminus

YTO17 Prp11-yEGFP
MATalpha, *prp2-1, ade2, his3, lys2-801, ura3*; *PRP11*::yEGFP-Ca*URA3* C-terminus

YTO18 Cwc24-yEGFP
MATalpha, *prp2-1, ade2, his3, lys2-801, ura3*; *CWC24*::yEGFP-Ca*URA3* C-terminus

YTO20 Cwc27-yEGFP
MATalpha, *prp2-1, ade2, his3, lys2-801, ura3*; *CWC27*::yEGFP-Ca*URA3* C-terminus

YTO21 Yju2-yEGFP
MATalpha, *prp2-1, ade2, his3, lys2-801, ura3*; *YJU2*::yEGFP-Ca*URA3* C-terminus

YTO25 Bud13-yEGFP
MATalpha, *prp2-1, ade2, his3, lys2-801, ura3*; *BUD13*::yEGFP-Ca*URA3* C-terminus

YOD224 Cwc24-TAP
MATalpha, *prp2-1, ade2, his3, lys2-801, ura3, CWC24*::TAP-K.I.*URA3* C-terminus

SC4160 Cwc27-TAP
MATa; ade2; arg4; leu2-3, 112; trp1-289; ura3-52; CWC27::TAP-K.I.*URA3* C-terminus (purchased from Euroscarf, Frankfurt am Main).

References

Boos DD. 2003. Introduction to the bootstrap world. *Statistical Science* **18**: 168-174.

Dertinger T, Pacheco V, von der Hocht I, Hartmann R, Gregor I, Enderlein J. 2007. Two-focus fluorescence correlation spectroscopy: a new tool for accurate and absolute diffusion measurements. *Chem Phys Chem* **8**: 433-443.

Fabrizio P, Dannenberg J, Dube P, Kastner B, Stark H, Urlaub H, Lührmann R. 2009. The evolutionarily conserved core design of the catalytic activation step of the yeast spliceosome. *Mol Cell* **36**: 593-608.

Földes-Papp Z. 2005. How the molecule number is correctly quantified in two-color fluorescence cross-correlation spectroscopy: corrections for cross-talk and quenching in experiments. *Curr Pharm Biotechnol* **6**: 437-444.

Földes-Papp Z, Rigler R. 2001. Quantitative two-color fluorescence cross-correlation spectroscopy in the analysis of polymerase chain reaction. *Biol Chem* **382**: 473-478.

Kettling U, Koltermann A, Schwille P, Eigen M. 1998. Real-time enzyme kinetics monitored by dual-color fluorescence cross-correlation spectroscopy. *Proc Natl Acad Sci U S A* **95**: 1416-1420.

Mütze J, Ohrt T, Schwille P. 2011. Fluorescence correlation spectroscopy in vivo. *Laser & Photonics Reviews* **5**: 52-67.

Ohrt T, Staroske W, Mutze J, Crell K, Landthaler M, Schwille P. 2011. Fluorescence cross-correlation spectroscopy reveals mechanistic insights into the effect of 2'-O-methyl modified siRNAs in living cells. *Biophys J* **100**: 2981-2990.

Puig O, Caspary F, Rigaut G, Rutz B, Bouveret E, Bragado-Nilsson E, Wilm M, Séraphin B. 2001. The tandem affinity purification (TAP) method: a general procedure of protein complex purification. *Methods* **24**: 218-229.

Ricka J, Binkert T. 1989. Direct measurement of a distinct correlation-function by fluorescence cross-correlation. *Physical Review A* **39**: 2646-2652.

Schwille P, Meyer-Almes FJ, Rigler R. 1997. Dual-color fluorescence cross-correlation spectroscopy for multicomponent diffusional analysis in solution. *Biophys J* **72**: 1878-1886.

Wahl M, Gregor I, Patting M, Enderlein J. 2003. Fast calculation of fluorescence correlation data with asynchronous time-correlated single-photon counting. *Opt Express* **11**: 3583-3591.

Warkocki Z, Odenwälder P, Schmitzová J, Platzmann F, Stark H, Urlaub H, Ficner R, Fabrizio P, Lührmann R. 2009. Reconstitution of both steps of Saccharomyces cerevisiae splicing with purified spliceosomal components. *Nat Struct Mol Biol* **16**: 1237-1243.

Yean SL, Lin RJ. 1991. U4 small nuclear RNA dissociates from a yeast spliceosome and does not participate in the subsequent splicing reaction. *Mol Cell Biol* **11**: 5571-5577.